ISSN1027-5495. Functional Materials, 31, No.3 (2024), p. 371-376
doi:http://dx.doi.org/10.15407/fm31.03.371

Densification, microstructure and hardness of middle entropy ceramics based on transition metals diboride

D. Vedel[1], P. Mazur[1], O. Grigoriev[1], I. Kozak[1], L. Melakh[1], M. Naumenko[2], M. Karpets[2], M. Skoryk[3], A. Zavdoveev[4]

[1] Frantsevich Institute for Problems in Materials Science, 3 Krzhizhanovsky St., 03142, Kyiv, Ukraine
[2] National Technical University of Ukraine "Igor Sikorsky Kyiv Polytechnic Institute", Peremogy Ave. 37, 03056 Kyiv, Ukraine
[3] Paton Electric Welding Institute of the NAS of Ukraine, 03150 Kyiv, Ukraine
[4] G. V. Kurdyumov Institute of Metal Physics of the NAS of Ukraine, NanoMedTech LLC, Kyiv, Ukraine

Received June 4. 2024

This article discusses the production and characterization of solid solutions based on single diboride phases, specifically TiB_2, ZrB_2, HfB_2, NbB_2, and TaB_2. These high-entropy ceramics TiB_2 denoted as (Ti, Zr, Hf)B_2, (Ti, Zr, Nb)B_2, and (Ti, Zr, Ta)B_2, were prepared through a meticulous process involving wet ball milling, hot pressing, and subsequent analysis. Microstructural analysis was conducted using scanning electron microscopy (SEM) and X-ray diffraction (XRD). The as-sintered ceramics had a complex microstructure, including solid solution − gray phase, (Hf, Zr)B_2 − white phase, and a dark phase formed during the polishing procedure. Chemical analysis using energy dispersive spectroscopy (EDS) indicated the formation of the $(Ti_{0.33}Zr_{0.33}Hf_{0.34})B_2$ solid solution in (Ti, Zr, Hf)B_2 ceramics. However, in the case of (Ti, Zr, Nb)B_2 and (Ti, Zr, Ta)B_2, inhomogeneous areas rich in Nb and Ta were observed, indicating the difficulty in achieving complete solubility in the AlB_2 structure. Hardness was measured at different indentation loads, and a decrease in hardness was revealed at higher loads. However, the high hardness observed at lower loads (200 H) for (Ti, Zr, Hf)B_2 solid solutions suggested a cocktail effect, similar to that observed in high-entropy metal alloys.

Keywords: Ddiborides, middle entropy ceramics, microstructure

Ущільнення, мікроструктура та твердість середньої ентропійної кераміки на основі диборидів перехідних металівю *Д. Ведель, П. Мазур, О. Григорьєв, І. Козак, Л. Мелах, М. Науменко, М. Карпець, М. Скорик, А. Завдовєєв*

У статті досліджено одержання та характеристики твердих розчинів на основі диборидів, зокрема TiB_2, ZrB_2, HfB_2, NbB_2 і TaB_2. Ці високоентропійні кераміки, позначені як (Ti, Zr, Hf)B_2, (Ti, Zr, Nb)B_2 і (Ti, Zr, Ta)B_2, були отримані у процесу, що включає мокре кульове подрібнення, гаряче пресування і подальше дослідження мікроструктури та механічних характеристик. Мікроструктурний аналіз проводили за допомогою скануючої електронної мікроскопії (СЕМ) та рентгенівської дифракції (РФА). Гаряче пресована кераміка мала складну мікроструктуру та включала твердий розчин − сіру фазу, (Hf, Zr)B_2 − білу фазу і темну фазу, утворену під час процедури шліфування. Хімічний аналіз з використанням енергодисперсійної спектроскопії показав утворення твердого розчину $(Ti_{0.33}Zr_{0.33}Hf_{0.34})B_2$ в кераміці (Ti, Zr, Hf)B_2. Однак у випадку (Ti, Zr, Nb)B_2 і (Ti, Zr, Ta)B_2 спостерігалися неоднорідні ділянки, багаті на Nb і Ta, що свідчить про труднощі в досягненні повної розчинності в структурі AlB_2. Вимірювання твердості проводили за різних навантажень, виявивши незначне зменшення твердості за великих навантажень. Однак висока твердість твердих розчинів (Ti, Zr, Hf)B_2, що спостерігається при менших навантаженнях (200 Н), свідчить про коктейльний ефект, подібний до того, що спостерігається у високоентропійних металевих сплавах.

1. Introduction

High-entropy ceramics are a rapidly developing class of materials that have gained significant interest in the materials science community due to their unique properties and potential for a wide range of applications. These ceramics are composed of multiple elements in nearly equal proportions, resulting in a complex, disordered crystal structure that contributes to their enhanced mechanical, thermal, and chemical properties [1]. Recent advances in materials science have led to the discovery and synthesis of several types of high-entropy ceramics, including oxides, carbides, nitrides, and borides. These materials have demonstrated exceptional properties, including high hardness, toughness, wear resistance, and thermal stability, making them promising candidates for use in various fields, such as aerospace, energy, and biomedical engineering [2].

High-entropy oxides are one of the most widely studied types of high-entropy ceramics. They have shown exceptional mechanical strength, high-temperature stability, and excellent oxidation resistance [3]. High-entropy carbides and nitrides are another important type of high-entropy ceramics. These materials have demonstrated excellent wear resistance, high hardness, and good thermal stability. Research has focused on the synthesis, characterization, and potential applications of high-entropy carbides and nitrides [4]. High-entropy borides are a relatively new type of high-entropy ceramics that have recently attracted attention due to their unique properties, including high hardness, high-temperature stability, and excellent oxidation resistance [5]. Research has focused on the synthesis and characterization of high-entropy borides, including their structure, properties, and potential applications [6].

Research on high-entropy ceramics has primarily focused on the synthesis and characterization of these materials, as well as their potential applications [7]. Various methods have been developed to synthesize high-entropy ceramics, including mechanical alloying, spark plasma sintering, and reactive sintering, among others. In addition, the properties of high-entropy ceramics were investigated using X-ray diffraction, electron microscopy and mechanical testing [8].

Diboride-based high-entropy ceramics have recently emerged as a new category of materials with unique properties and potential applications. Diborides are composed of boron and another metal or metalloid element, have high melting points, excellent electrical conductivity, and high hardness, making them suitable for use in various high-temperature and high-wear applications [9]. The synthesis of diboride-based high-entropy ceramics involves the addition of multiple elements in nearly equal proportions to create a disordered and complex crystal structure, resulting in materials with enhanced properties compared to diborides alone [10]. Recent research has focused on synthesizing diboride-based high-entropy ceramics and investigating their properties. For example in [11], SiC-HfB_2-ZrB_2 high-entropy ceramic composites with high hardness and good thermal stability were synthesized. The microstructure and properties of high-entropy ceramic coatings based on HfB_2 and ZrB_2 for cutting tools and found that they showed excellent wear resistance and high hardness were investigated.

The unique properties of diboride-based high-entropy ceramics make them promising candidates for a wide range of applications. For instance, they could be used in aerospace, energy, and cutting tools, where high temperature and wear resistance are crucial. The potential

Table 1 – Characteristics of the raw powders

Powder	Average grain size, μm	Lattice constant, nm		Oxygen content, wt. %	Factory
		"a"	"c"		
TiB_2	3.9	0.30299	0.32287	1.2	Donetsk plant, Ukraine
ZrB_2	3.3	0.31680	0.35305	0.8	Eno Material Co., Ltd., China,
HfB_2	6.1	0.31411	0.34751	1.5	Donetsk plant, Ukraine
NbB_2	6.5	0.30998	0.33006	1.2	Donetsk plant, Ukraine
TaB_2	19.3	0.30880	0.33430	1.4	Donetsk plant, Ukraine

Table 2 – Chemical composition, temperature of HP, holding time, phase composition, average grain size, microhardness and lattice constants of solid solutions

Solid solution	Temperature of HP, oC	Holding time, min	Average grain size of solid solution, μm	Microhardness, GPa			Lattice constant		Ref
				$Hv_{0.2}$	Hv_2	Hv_{200}	"a", nm	"c", nm	
$(Ti,Zr,Hf)B_2$	2100	30	5.5±1.8	-	20.8	18.5	0.31141	0.34257	
$(Ti,Zr,Nb)B_2$	2100	30			22.2	15.3	0.30958	0.33558	
$(Ti,Zr,Ta)B_2$	2100	30			25.3	19.8	0.30892	0.33406	
$(Ti, Zr, Hf, Ta, V)B_2$	2100	10	7.7±3.2	28.3±0.5	–	–	0.30858	0.33464	[13]
$(Ti, Zr, Hf, Ta, Cr)B_2$	2000	10	3.2±1.3	32.9±2.7	–	–	0.30824	0.33502	[13]
$(Ti, Zr, Hf, Ta, Nb)B_2$	2100	10	4.9±2.4	25.2±0.6	–	–	0.31053	0.33779	[13]
$(Ti, Zr, Hf, Ta, Mo)B_2$	2000	10	15.9±7.0	30.6±3.4	–	–	0.30915	0.33779	[13]
$(Ti, Zr, Hf, Ta, W)B_2$	2100	10	9.3±3.5	34.8±1.2	–	–	0.30930	0.33535	[13]
$(Ti, Zr, Hf, Mo, W)B_2$	2000	10	13.4±5.5	30.9±0.8	–	–	0.30828	0.33468	[13]
$(Ti, Zr, Hf, Nb, Ta)B_2$	2000	5	–	17.5±1.2	–	–	0.3101	0.3361	[15]
$(Ti, Zr, Hf, Cr, Ta)B_2$	2000	5	–	19.9±2.6	–	–	0.3079	0.3336	[15]
$(Ti, Zr, Hf, Cr, Ta)B_2$	2000	10	–	~29	–	–	0.3089	0.3362	[30]
$(Ti, Zr, Hf, Mo, W)B_2$	2000	10	14.7±12.4	26.0±1.5	–	–	0.3079	0.3338	[31]
$(Ti, Zr, Hf, Mo, W)B_2$	2000	30	4.3±1.8	29.4±1.7	–	–	0.3084	0.3357	[32]

applications of diboride-based high-entropy ceramics have prompted further research to understand their properties and develop new synthesis techniques.

In summary, high-entropy ceramics are a promising class of materials with unique properties that have attracted significant interest in the materials science community. Further research and development are required to fully understand the potential of these materials and to explore their diverse applications in different fields.

The purpose of present study was to investigate the influence of hot pressing (HP) parameters on the structure and hardness of low, middle entropy ceramics based on transition metals diboride (TiB_2, ZrB_2, HfB_2, NbB_2 and TaB_2).

2. Experimental

The single-phase diborides TiB_2, ZrB_2, HfB_2, NbB_2 and TaB_2 were used to produce solid solutions with different compositions (Table 1, Table 2). The middle entropy ceramics $(Ti, Zr, Hf)B_2$, $(Ti, Zr, Nb)B_2$, $(Ti, Zr, Ta)B_2$ were mixed by wet ball milling in a PET crucible using a 1-5 mm WC-6Co grinding medium in acetone, with rotation speed of 400 rpm for 5 h. The wet powder mixtures were dried by rotary evaporator and sieved through a 60 mesh. The powder mixtures were directly poured in a graphite die previously coated with boron nitride. The heating rate was 100°C/min to the

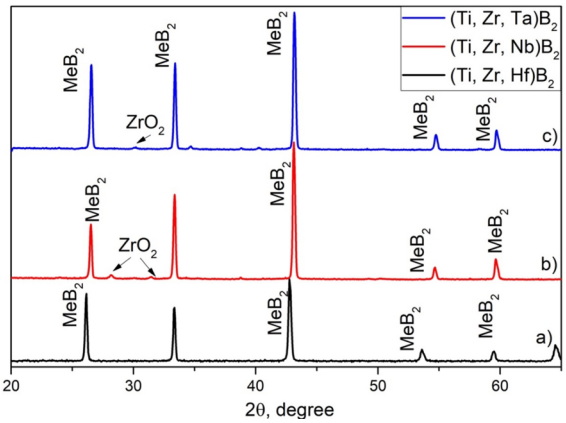

Fig. 1 – XRD patterns of HP ceramics: a-$(Ti, Zr, Hf)B_2$; d-$(Ti, Zr, Nb)B_2$; c-$(Ti, Zr, Ta)B_2$

densification temperature, followed by holding at the temperature for 30 min and cooling at a rate of 100-200°C/min. The consolidation was carried out by hot pressing (HP) in a CO/CO_2 atmosphere. The densification conditions and properties of the produced ceramics are summarized in Table 2.

The structure of sintered ceramics was studied by scanning electronic microscopy using a Mira 3 instrument (Tescan Co., Czech Republic) with acceleration voltage of 10 and 20 keV with an energy dispersive spectroscopy EDS detector Oxford X-Max (INCA, Oxford instruments, UK). A Rigaku Ultima IV, (Japan) diffractometer was used to study the crystalline phase composition.

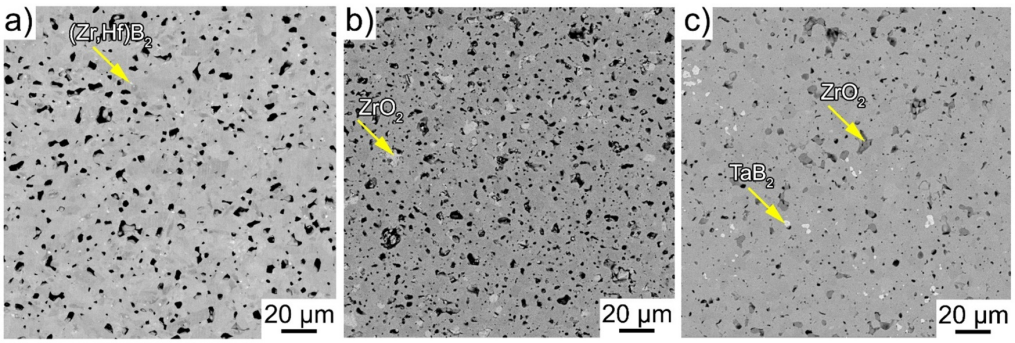

Fig. 2 – Microstructure of ceramics obtained by HP: a – (Ti, Zr, Hf,)B_2; b – (Ti, Zr, Nb)B_2, c – (Ti, Zr, Ta)B_2

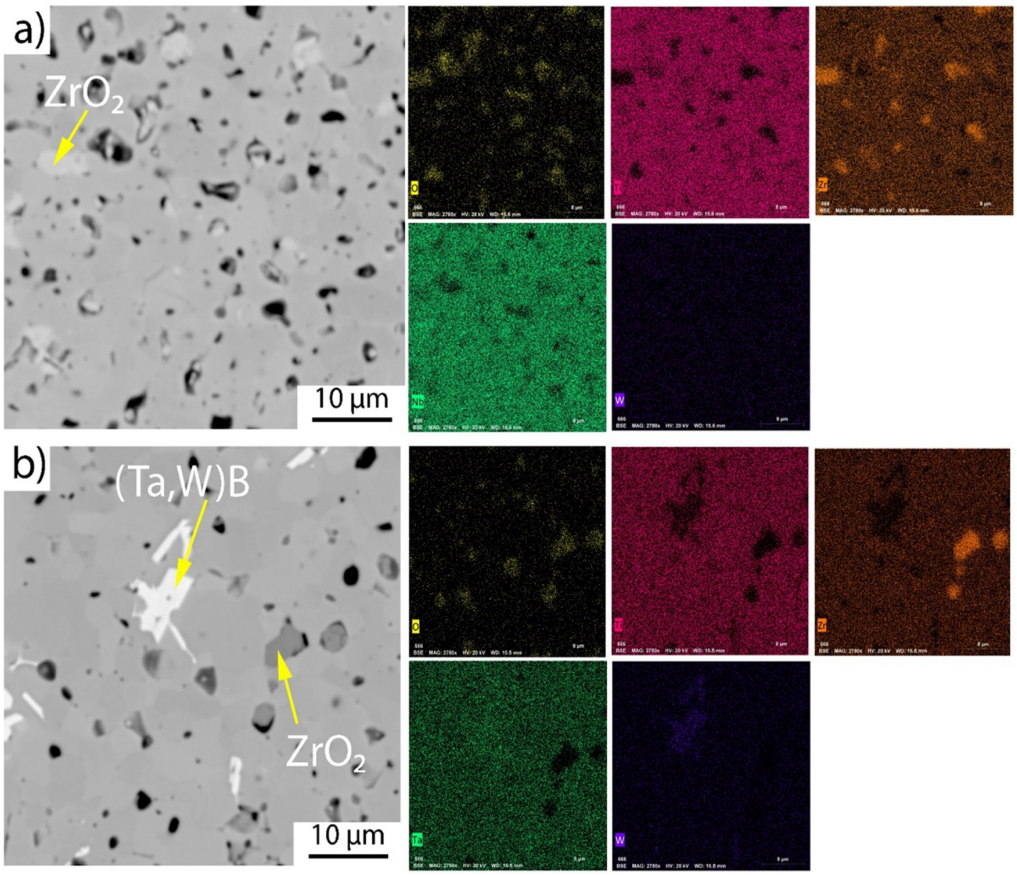

Fig. 3 – Microstructure of HP ceramics (Ti, Zr, Nb)B_2 (a) and (Ti, Zr, Ta)B_2 at 2100 °C with distribution of map elements

3. Results and Discussion

Microstructures of ternary systems consist of a solid solution-gray phase, inclusions of (Hf, Zr)B_2 – a white phase, and a dark phase (Figs. 1, 2). The dark phase represented grains that fell out during the polishing procedure. The XRD spectra (Fig. 1 a) and SEM images (Fig. 2 b) indicate the formation of (Ti, Zr, Hf)B_2 solid solutions. It can be explained by similar atomic radii of the metals Ti (1.43 Å), Zr (1.59 Å), Hf (1.56 Å). According to EDS analysis, the chemical formula of the solid solution was ($Ti_{0.33}Zr_{0.33}Hf_{0.34}$)$B_2$ (Fig.2).

A slightly different situation was observed for (Ti, Zr, Nb)B_2 and (Ti, Zr, Ta)B_2 composites. Along with the solid solution, ZrO_2 and W-Ta-B phases were observed (Fig 2). According to the EDS analysis, the chemical compositions of the solid solutions were ($Ti_{0.45}$, $Zr_{0.26}$, $Nb_{0.32}$)B_2 and ($Ti_{0.5}$, $Zr_{0.35}$, $Ta_{0.15}$)B_2. Monteverde et al. [12, 13] observed the Nb- and Ta- rich regions in (Ti, Zr, Hf, Nb, Ta) B_2. These regions were observed only when the acceleration energy

was more than 10 keV. At energies of 10 keV or below, the amount of signal generated was small, allowing the segregation of Ta or Nb to be observed. In our case, a similar region rich in Nb and Ta was observed for these four solid solution compounds (Fig. 3). We assume that the inhomogeneous regions were formed due to incomplete solubility of metals in the metallic sublattice of the AlB_2 structure.

The average grain size of solid solutions depends on two major factors: (i) temperature of HP; (ii) phase composition. On the one hand, the low temperature of HP (1900-1950 °C) resulted in the formation of fine grains of solid solution ~ 3-4 μm with the simultaneous presence of HfB_2 in the microstructure (Table 2). On the other hand, at the optimum HP temperature (2000-2100 °C) for the formation of a homogenous solid solution, the grain size was 5-7 μm (Table 2). In terms of composition, the system requiring low temperature to form a complete solid solution (Ti, Zr, Hf)B_2, has a finer grain size compared to (Ti, Zr, Nb)B_2 and (Ti, Zr, Ta)B_2.

In the preparation of the transition metal diboride based solid solution, three main problems were considered: (i) densification; (ii) homogeneity of the solid solution; (iii) properties.

The high entropy solid solution based on diborides can be densified at ~ 1950°C. At lower temperatures, complete densification of ceramics and obtaining solid solution was impossible. Dymirsky et al. [14] describe the formation of two solid solutions in the (Zr, Hf, Ta)B_2 ceramics at the lower temperature of densification (1800°C) or a short holding time (1 min). Increasing the densification temperature to 1927°C and holding time to 20 min resulted in a pure and dense solid solution. This indicates that the HP temperature plays a major role in the formation of the solid solution.

As we mentioned above, the inhomogeneous regions were observed in all solid solutions. The Ta- and Nb- rich regions were formed in the technological process of obtaining a solid solution as a result of densification of monometallic diboride [15] or reduction of metal oxide with B_4C, B, B+C [16–18]. Gu et al. [19] reported that boron deficiency resulted in significant segregation during solid solution formation. According to the phase diagram, this is due to the formation of Me_xB_y phases based on Nb and Ta. Me_xB_y phases have a different crystal structure compared to MeB_2 and cannot dissolve in the diboride solid solution. However, in our case, the content of boron in Ta- or Nb- rich phases was ~ 66 at.%. Zhang [20] suggested that the segregation of Nb is due to the lower chemical stability of Nb–B compared with other metal-boron compounds due to the enhanced hybridization between the metal and B [21]. Fahrenholtz et al. [22] showed that that the formation of solid solutions of diborides depends significantly on the activation energy of metal diffusion. We suggest that the main reason of the segregation lays in metallic sub-layer in AlB_2 lattice. Another important reason is the formation of phases Ti-W-B and ZrO_2 phase. The Ti-W-B phase was formed due to interaction between WC and TaB_2 during hot pressing. ZrO_2 was present in the composition because ZrB_2 interacts with surrounding oxygen in the nearest phases, since it has the highest affinity to oxygen.

Hardness. Monteverde et al. [13] have shown that hardness of high entropy ceramics based on diborides of transition metals strongly depends on the indentation load. At the indentation load of 10 H, the hardness was in range of ~ 21.0 – 25.4 GPa. In our case, a more significant decrease of hardness is observed at a load of 200 H (Table 2). *Our composite* exhibits high hardness (>17 GPa) at an indentation load of 200 N.

We assume that, the high hardness of the (Ti,Zr,Hf)B_2 solid solution is due to the highest hardness of TiB_2 [23]. The similar cocktail effect was observed on the high entropy metal alloys [13].

Depending on the test conditions, the reported hardness for TiB_2 varies from 26.6 to 38.2 GPa [13]. Riley and Niiler's [24] measurements of hardness under the same load (0.1 kg) ranged from 17.6 to 25.6 GPa for SHS/DC TiB_2 and from 24.5 to 34.3 GPa for hot-pressed TiB_2. The TiB_2 hardness determined by Honak [25] under a load of 0.1 kg, was 33.3 GPa. Addition of TiB_2 particles can greatly increase the microhardness.

In [26], the hardness of ZrB_2 is reported to be up to 23 GPa, while in [27] the hardness of HfB_2 is 40.7 GPa. The hardness of NbB_2 [28] and TaB_2 [29] were 35.8 and ~30 GPa, respectively.

The hardness of the starting materials is ~26 GPa, while for the entropic materials it reached up to 30 GPa. Comparing the hardness of individual materials such as TiB_2, ZrB_2, HfB_2, NbB_2, and TaB_2 with the data in Table 2, it becomes clear that the hardness increases depending on the fifth component.

4. Conclusions

1. The homogeneous solid solution was formed in the (Ti, Zr, Hf)B_2 system.

2. The Ta- and Nb-rich regions were observed in (Ti, Zr, Nb)B_2 and (Ti, Zr, Ta)B_2 solid solutions. This segregation was associated with boron deficiency, resulting in the formation of Me_xB_y phases based on Nb and Ta. Furthermore, increased hybridization between metal and B, low chemical stability of Nb–B, and activation energy of metal diffusion were identified as factors influencing segregation.

3. The hot pressing influences on the phase composition and grain size of solid solutions. Lower HP temperatures (1900-1950°C) led to fine grains (~3-4 μm), while at the optimum HP temperatures (2000-2100°C), the larger grains (5-7 μm) were formed.

References

1. V.E. Álvarez-Montaño, M. Kumar, S. Sharma, R. Kumar Chourasia, P. Kumar, J.M. Siqueiros, O. Raymond Herrera, *Mater Lett* **349** (2023)
2. Nam, Prediction of mechanical properties of high-entropy ceramics by deep learning with compositional descriptors, *Mater Today Commun* **35** (2023)
3. M. Anandkumar, E. Trofimov, *J Alloys Compd* **960** (2023)
4. Q. Zhou, F. Xu, C. Gao, W. Zhao, L. Shu, X. Shi, M.F. Yuen, D. Zuo, *Ceram Int* **49** (2023)
5. Y. Zhang, Z. Bin Jiang, S.K. Sun, W.M. Guo, Q.S. Chen, J.X. Qiu, K. Plucknett, H.T. Lin, *J Eur Ceram Soc* **39** (2019)
6. S. Kavak, K.G. Bayrak, M. Mansoor, M. Kaba, E. Ayas, Ö. Balcı-Çağıran, B. Derin, M.L. Öveçoğlu, D. Ağaoğulları, *J Eur Ceram Soc* **43** (2023)
7. An original source: S. Akrami, P. Edalati, M. Fuji, K. Edalati, High-entropy ceramics: Review of principles, production and applications, Materials Science and Engineering: R: Reports 146 (2021)
8. R.Z. Zhang, M.J. Reece, High-Entropy Ceramics, Encyclopedia of Materials: Metals and Alloys (2022)
9. R.F. Guo, H.R. Mao, P. Shen, *J Eur Ceram Soc* **43** (2023)
10. P.H. Mayrhofer, A. Kirnbauer, P. Ertelthaler, C.M. Koller, *Scr Mater* **149** (2018)
11. A. Nisar, M.M. Khan, S. Bajpai, K. Balani, *Int J Refract Metals Hard Mater* **81** (2019)
12. F. Monteverde, F. Saraga, M. Gaboardi, J.R. Plaisier, *J Eur Ceram Soc* **41** (2021)
13. L. Feng, F. Monteverde, W.G. Fahrenholtz, G.E. Hilmas, *Scr Mater* **199** (2021). https://doi.org/10.1016/j.scriptamat.2021.113855.
14. D. Demirskyi, T.S. Suzuki, K. Yoshimi, O. Vasylkiv, *J.Ceramic Society of Japan* **128** (2020)
15. J. Gild, Y. Zhang, T. Harrington, S. Jiang, T. Hu, M.C. Quinn, W.M. Mellor, N. Zhou, K. Vecchio, J. Luo, *Sci Rep* **6** (2016)
16. D. Liu, T. Wen, B. Ye, Y. Chu, *Scr Mater* **167** (2019)
17. L. Feng, W.G. Fahrenholtz, G.E. Hilmas, *Journal of the American Ceramic Society* **103** (2020)
18. S. Failla, P. Galizia, S. Fu, S. Grasso, D. Sciti, *J Eur Ceram Soc* **40** (2020)
19. J. Gu, J. Zou, S.K. Sun, H. Wang, S.Y. Yu, J. Zhang, W. Wang, Z. Fu, *Sci China Mater* **62** (2019)
20. Y. Zhang, S.K. Sun, W. Zhang, Y. You, W.M. Guo, Z.W. Chen, J.H. Yuan, H.T. Lin, *Ceram Int* **46** (2020)
21. W.G. Fahrenholtz, E.J. Wuchina, W.E. Lee, Y. Zhou, Ultra-High Temperature Ceramics Materials for Extreme Environment Applications, John Wiley & Son, 2014.
22. W.G. Fahrenholtz, J. Binner, J. Zou, *J Mater Res* **31** (2016)
23. G. V. Samsonov, I. Vinitskiy, Refractory Compounds, 1976.
24. D.J. Hepner, K.P. Soencksen, B.S. Davis, N.G. Maiorana, 938-Serving the Army for Fifty Years-1988 BRL INTERNAL PRESSURE MEASUREMENTS FOR A LIQUID PAYLOAD AT LOW REYNOLDS NUMBERS, n.d.
25. L. Wang, M.R. Wixom, L.T. Thompson, Structural and mechanical properties of TiB2 and TiC prepared by self-propagating high-temperature synthesis/dynamic compaction, 1994.
26. M.S. Asl, M.G. Kakroudi, S. Noori, *J Alloys Compd* **619** (2015)
27. Y. Pan, H. Huang, X. Wang, Y. Lin, *Comput Mater Sci* **109** (2015)
28. M. Upatov, J. Vleugels, Y. Koval, V. Bolbut, I. Bogomol, Microstructure and mechanical properties of B4C-NbB2-SiC ternary eutectic composites by a crucible-free zone melting method, n.d.
29. X. Zhang, G.E. Hilmas, W.G. Fahrenholtz, *Mater Lett* **62** (2008)
30. Y. Zhang, S.K. Sun, W.M. Guo, W. Zhang, L. Xu, J.H. Yuan, D.K. Guan, D.W. Wang, Y. You, H.T. Lin, *J Eur Ceram Soc* **41** (2021)
31. M. Qin, J. Gild, H. Wang, T. Harrington, K.S. Vecchio, J. Luo, *J Eur Ceram Soc* **40** (2020)
32. J. Gild, A. Wright, K. Quiambao-Tomko, et al *Ceram Int* **46** (2020)